Soret and Dufour effects on entropy generation for AIN and Al_2O_3 Hybrid Nanofluid Flow over past a stretching sheet in porous media

Motahar Reza[1], Anindita Bhattacharyya[2], and Amalendu Rana[3,] and Raghunath Patra[4]

[1]School of Computer Science and Engineering

[1,3]Department of Mathematics, National Institute of Science & Technology.Berhampur-761008, Odisha, India.

[2]Department of Mathematics ,Amity University, Kolkata-700135, West Bengal, India

[3,4] Department of Mathematics, Berhampur University, Berhampur-760007, Odisha, India,

[1]reza@nist.edu, [2]aninmb@gmail.com, [3]amalmath94@gmail.com, [4]raghunathpatra09@gmail.com

ABSTRACT

The numerical investigation on Soret and Duffer effects on entropy generation for ($AIN - Al_2O_3$) Hybrid Nanofluid flow past over a stretching plate through hybrid nano-fluid- saturated porous medium. The transvers magnetic field has been applied to examine the effect of Soret and Duffer on entropy generation for this problem. Mixture of Aluminum Nitride (AIN) and Alumina nanoparticles(Al_2O_3)nanoparticles with base fluid water has been used to investigate the enhancement of heat transfer rates. This new fluid flow model is cleated to examine the thermal radiation and viscous dissipation effect in the presence of magnetic fluid . It is interesting to note that chemical reaction and heat transfer rate for this nanofluid is higher than the simple nanofluid.

Keywords: Soret and Duffer effects, Hybrid nanofluid, Porous medium, Stretching sheet.

1. INTRODUCTION

Space technology and process involving high temperature. Soret and Dufour effects are very significant for the fluids which have higher temperature and Nanofluids are a classification of heat transfer fluids which are engineered suspension nanoparticles (1–100 nm) being dispersed in the fluid. Usually base fluids incorporate water, organic fluids (e.g. ethylene, triethylene and so on) engine oil, polymeric solutions, bio-fluids and other basic fluids. Medium normally utilized as nanoparticles encompass carbon in different structures (e.g. carbon nanotubes, graphite, diamond) metals (e.g. copper, silver, gold), metal oxides (e.g titania, zirconia) and functionalized nanoparticles. Although these types of conventional nano-fluids have huge application in industry, many researchers and designers are recognized in studying the heat transfer enhancement in the last decades in order to remove the generation of heat in flow structure. Hybrid nanofluids are a new class of working fluids containing very small particles with sizes (under 100 nm) used in heat transfer applications. These fluids consist from two or three solid materials dispersed in conventional fluids. Many of heat transfer enhancement studies utilizing

various nanofluids type such as $Al_2\ O_3$, CNT, Cu, Fe_2O_3, Ag, CuO, TiO_2, SiO_2, ZnO and SiC through a tube have been done [1-3]. The hybrid nano-fluids leads to an increased thermal conductivity and finally to a heat transfer enhancement in heat exchangers.

Thermal radiation plays very significant role in the surface heat transfer when convection heat transfer is very small. Also, the effects of thermal radiation on forced and free convection flow are important in the content of concentration gradients and these are also important in macroscopically physical phenomenon in fluid mechanics [4]. The thermo-diffusion (Soret) effect corresponds to species differentiation developing in an initial homogeneous mixture submitted to a thermal gradient and the diffusion-thermo (Dufour) effect corresponds to the heat flux produced by a concentration gradient. Usually, in heat and mass transfer problems, the variation of density with temperature and concentration give rises to a combined buoyancy force under natural convection and hence, the temperature and concentration will influence the diffusion and energy of the species. The applications of Soret and Dufour effects can be found in the area of reactor safety, combustion flames and solar collectors as well as building energy conservation

In recent years, the efficiency calculation of the heat exchanger systems was restricted to the first law of thermodynamics in many studies. Entropy generation minimization method has been comprehensively covered by Bejan[5] specifically which is basically employed to optimize the thermal engineering devices for higher energy efficiency. In order to access the best design of thermal systems, one can employ the second law of thermodynamics by minimizing the irreversibility. The performance of engineering equipment in the presence of the irreversibilities is reduced and entropy generation function is a measure of the level of the available irreversibilities in a process [6-7].

The objective of this work is to study the Soret and Duffer effects on the hybrid nano-fluid (mixture of Aluminium Nitride (AIN) and Alumina nanoparticles(Al_2O_3) with base fluid water) flow in the presence of magnetic field . This results impact the entropy generation which can controlled by applied transfer magnetic field. Rate of heat transfer enhancement of this hybrid nano fluid can be controls by applied magnetic field.

1.1. Hybrid nano-fluid Properties:

The equivalent thermal properties density, thermal conductivity, specific heat and viscosity of hybrid nano fluid have been calculated by using the following formulas [6].

$$\rho_{hnf} = \left(\frac{\phi}{100}\right)\rho_P + \left(1 + \frac{\phi}{100}\right)\rho_F;$$

$$\frac{k_{hnf}}{k_F} = 1.2035\left\{\left(0.001 + \frac{\phi}{100}\right)^{0.0098}\left(0.01 + \frac{T_{hnf}}{90}\right)^{0.1331}\left(0.001 + \frac{dp}{170}\right)^{-0.0001}\left(0.01 + \frac{\alpha_P}{\alpha_F}\right)^{0.0153}\right\}$$

$$(\rho C_P)_{hnf} = \left(\frac{\phi}{100}\right)(\rho C_P)_P + \left(1 - \frac{\phi}{100}\right)(\rho C_P)_F;$$

$$\frac{\mu_{hnf}}{\mu_F} = 0.3659 \times C1 \times \exp\left\{\left(1 + \frac{\phi}{100}\right)^{10.83}\left(\frac{T_{hnf}}{90}\right)^{-0.0239}\left(1 + \frac{dp}{170}\right)^{-0.1609}\right\};\ \alpha_{hnf} = \frac{k_{hnf}}{(\rho C_p)hnf}\ ,$$

$$\nu_F = \frac{\mu_F}{\rho_F}.$$

Where ϕ is the hybrid nano fluid nano particle volume fractions and symbol subscripts F, P and hnf are referred to fluid, solid nanocomposite particles and hybrid nano fluid respectively.

Table: Nanoparticles and basefluid thermal properties [7].

Properties	Water	Al_2O_3	AIN
Density(kg/m^3)	998	3880	3260
Specific heat(J/kg.K)	4180	773	735
Thermal conductivity(W/m.K)	0.6067	40	180
Viscosity (kg/m.s)	0.0014	-	-

2. PROBLEM DESCRIPTION AND MATHEMATICAL MODELING

The steady Hybrid nanofluid flow over a vertical stretching sheet via hybrid nanofluid- saturated porous medium has been assumed as displayed in Fig.1. X-axis is taken along the stretching

surface and y-axis is put perpendicular to the stretching surface. The transverse magnetic field $\boldsymbol{B} = (0, B_0, 0)$ has applied to perpendicular to the plate. The flow is considered to be bounded by $y > 0$.

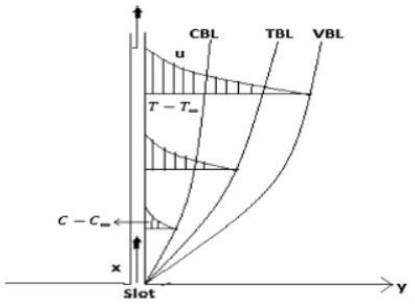

Figure 1: Sketch of the Physical Problem

The governing equations for momentum , temperature and concentration to considering thermal reaction, viscous dissipation and Soret and Dufour effects are expressed in the following form

$$\frac{\partial u}{\partial x} + \frac{\partial v}{\partial y} = 0 \tag{1}$$

$$u\frac{\partial u}{\partial x} + v\frac{\partial u}{\partial y} = \frac{\mu_{hnf}}{\rho_{hnf}}\frac{\partial^2 u}{\partial y^2} - \frac{\mu_{hnf}}{\rho_{hnf}}\frac{1}{K}u - \frac{1}{\rho_{hnf}}\sigma B_0^2 u \tag{2}$$

$$u\frac{\partial T}{\partial x} + v\frac{\partial T}{\partial y}\alpha_{hnf}\frac{\partial^2 T}{\partial y^2} - \frac{1}{\left(\rho c_p\right)_{hnf}}\frac{\partial q_r}{\partial y} + \frac{\mu_{hnf}}{\left(\rho c_p\right)_{hnf}}\left(\frac{\partial u}{\partial y}\right)^2 + \frac{\mu_{hnf}}{(\rho C_P)_{hnf}}\frac{u^2}{K} + \frac{1}{\left(\rho c_p\right)_{hnf}}\frac{\partial q_r}{\partial y} + \frac{1}{(\rho C_P)_{hnf}}(q_H''') + \frac{D_2}{(\rho C_P)_{hnf}}\frac{\partial^2 C}{\partial y^2} \tag{3}$$

$$u\frac{\partial C}{\partial x} + v\frac{\partial C}{\partial y} = D_m\frac{\partial^2 C}{\partial y^2} + D_1\frac{\partial^2 T}{\partial y^2} - K_0(C - C_\infty) \tag{4}$$

The boundary Conditions can be written as

$$u = U_w(x) = ax,\ v = 0, T = T_w, C = C_w\ at\ y = 0 \tag{5}$$

$$u \to 0;\ T \to T_\infty;;\ C \to C_\infty as\ y \to \infty$$

For Similarity transformation and making dimensionless, we consider:

$$\psi = \sqrt{a\nu_F}\, x\, F_h(\eta)\,,\ u = axF_h'(\eta)\ ,\ v = \sqrt{a\nu_F}F_h(\eta)\ ,\ \eta = \sqrt{\frac{a}{\nu_F}}\, y\,;\, \theta_h = \frac{T - T_\infty}{T_w - T_\infty}\,, \phi_h = \frac{C - C_\infty}{C_w - C_\infty}$$

The non-uniform heat sourse/sink, is defined by

$$q_H''' = \frac{k_{hnf}a}{\nu_F}\{A(T_w - T_\infty)F_h' + B(T - T_\infty)\} \quad (6)$$

where A and B are the space and temperature dependent heat source/sink respectively.

The momentum and Energy equations are reduced as

$$F_h''' + A_1A_2\left\{F_hF_h'' - (F_h')^2 - \frac{M}{A_2}F_h'\right\} - K_P^*F_h' = 0 \quad (7)$$

$$\left(1 + \frac{An}{A_5}\right)\theta_h'' + \frac{Pr}{A_5}\left[A_3F_h\theta_h' + \frac{Ec}{A_1}\{K_P^*(F_h')^2 + (F_h'')^2\} + A_5(A_1^*F_h' + B_1^*\theta_h) + Du\,\phi_h''\right] = 0 \quad (8)$$

$$\phi_h'' + Sc\,(F_h\phi_h' + Sr\theta_h'' - C_1^*\phi_h) = 0 \quad (9)$$

where $M = \frac{\sigma B_0}{\rho_F a}$Magnetic parameter.$K_P^* = \frac{\nu_F}{Ka}$ Porous medium parameter. $Pr = \frac{\nu_F}{\alpha_F}$ Prandtl number. $A_1^* = \frac{Ak_F}{(\rho C_P)_F}$ Heat source /sink (space dependent). $B_1^* = \frac{Bk_F}{(\rho C_P)_F}$ Heat source /sink (temperature dependent). $Ec = \frac{U_w^2}{(C_P)_F}\frac{1}{(T_W - T_\infty)}$Eckert number. $Du = \frac{D_2(C_W - C_\infty)}{a(\rho C_P)_F(T_W - T_\infty)}$ Dufour number. $An = \frac{4T_\infty^3\sigma^*}{3k^*k_F}$ radiation parameter.$Sc = \frac{\nu_F}{D_m}$ Schmidt number. $Sr = \frac{D_1(T_W - T_\infty)}{\nu_F(C_W - C_\infty)}$ Soret number. $C_1^* = \frac{K_0}{a}$ chemical reaction parameter.

$\frac{1}{A_1} = 0.3659 \times C1 \times \exp\left\{\left(1 + \frac{\phi}{100}\right)^{10.83}\left(\frac{T_{hnf}}{90}\right)^{-0.0239}\left(1 + \frac{dp}{170}\right)^{-0.1609}\right\}$;$A_2 = \left(\frac{\phi}{100}\right)\frac{\rho_P}{\rho_F} + \left(1 + \frac{\phi}{100}\right)$; $A_3 = \left(\frac{\phi}{100}\right)\frac{(\rho C_P)_P}{(\rho C_P)_F} + \left(1 - \frac{\phi}{100}\right)$; $A_5 = 1.2035\left\{\left(0.001 + \frac{\phi}{100}\right)^{0.0098}\left(0.01 + \frac{T_{hnf}}{90}\right)^{0.1331}\left(0.001 + \frac{dp}{170}\right)^{-0.0001}\left(0.01 + \frac{\alpha_P}{\alpha_F}\right)^{0.0153}\right\}$.

Boundary conditions are reduced to

$$F_h = 0; F_h' = 1; \theta_h = 1; \phi_h = 1 \quad at\ \eta = 0 \quad (10)$$

$$F_h' = 0; \theta_h = 0; \phi_h = 0 \quad at\ \eta \to \infty$$

2.1.Entropy generation analysis:

According [4, 5] , the volumetric rate of local entropy generation of hybrid nanofluid over the stretching surface can be written as

$$S_{gen}^{m} = \frac{k}{T_\infty^2}\left(\frac{\partial T}{\partial y}\right)^2 + \frac{\mu}{T_\infty^2}\left(\frac{\partial u}{\partial y}\right)^2 + \frac{RD}{C_\infty}\left(\frac{\partial C}{\partial y}\right)^2 + \frac{RD}{T_\infty}\frac{\partial T}{\partial y}\frac{\partial C}{\partial y} \tag{11}$$

The dimensionless entropy generation number (N_G) becomes:

$$N_G = \frac{S_{gen}^{m}}{S_0^{m}} = Re\{A_5(\theta_h')^2 + \frac{Br}{A_1\alpha^*}(F_h'')^2 + \lambda^*\left(\frac{\beta^*}{\alpha^*}\right)^2(\phi_h')^2 + \lambda^*\left(\frac{\beta^*}{\alpha^*}\right)\theta_h'\phi_h' \tag{12}$$

where $\lambda^* = \frac{RDC_\infty}{k_F}$ is the diffusive constant.$Br = \frac{\mu_F U_W^2}{k_F \Delta T}$ Brinkman number. $\alpha^* = \frac{\Delta T}{T_\infty}$, $\beta^* = \frac{\Delta C}{C_\infty}$ are the dimensionless temperature and concentration differences.$S_0^m = \frac{k_F(\Delta T)^2}{L^2 T_\infty^2}$ is the characteristics entropy generation rate.$Re = \frac{u_L L}{\nu_F}$ Reynolds number.

3. RESULTS AND DISCUSSIONS

The nonlinear differential equations (7-9) which represent the velocity distribution, temperature distribution and concentration respectively, along with the respective boundary conditions (10) are solved numerically using the Runge-Kutta fourth order method along with shooting technique. In order to solve these nonlinear higher order equations firstly, they were reduced to a set of first order differential equations. Then, the suitable guesses were passed to the function as the initial solution. The computations were done for a mesh size of 100-500 and the tolerance limit was set to .001. The results of the comprehensive numerical study are illustrated geometrically in this section with the parameter values $M = 0.5, K_P^* = 0.5; An = 0.2; A_1^* = B_1^* = -0.1; C_1^* = 0.1; Sc = 1; Sr = 1; Ec = 0.1; Du = 0.2; Pr = 6.2; Re = 2; Br = 10.$ Also, the effects of various pertinent parameters on the velocity, temperature, concentration and entropy generation profiles are represented in this section.

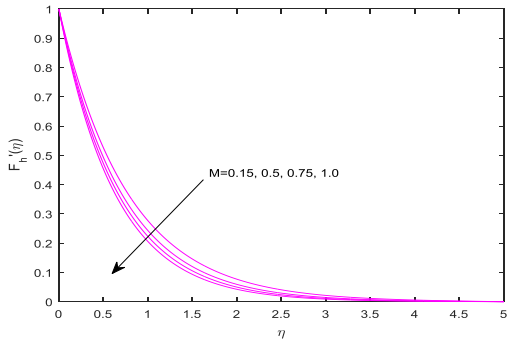

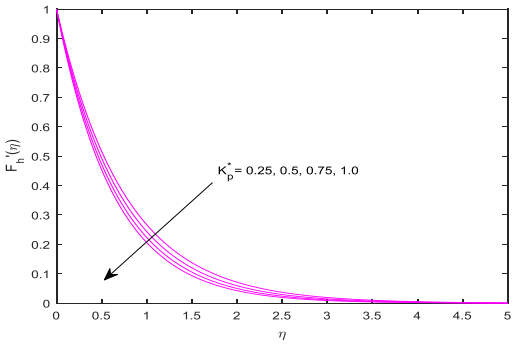

(a) (b)

Figure 2. (a)Effect of magnetic parameter, (b) effect of porous medium parameter on velocity profile.

The effects of magnetic parameter and porous medium parameter on the velocity profiles are depicted in figure 2. The enhancement of the magnetic parameter and the porous medium parameter reduce the velocity profile which are shown in figure 2(a) and 2(b) respectively. In the figure 2(a) the velocity is decreased due to the Lorentz force which acts as a retarding force.

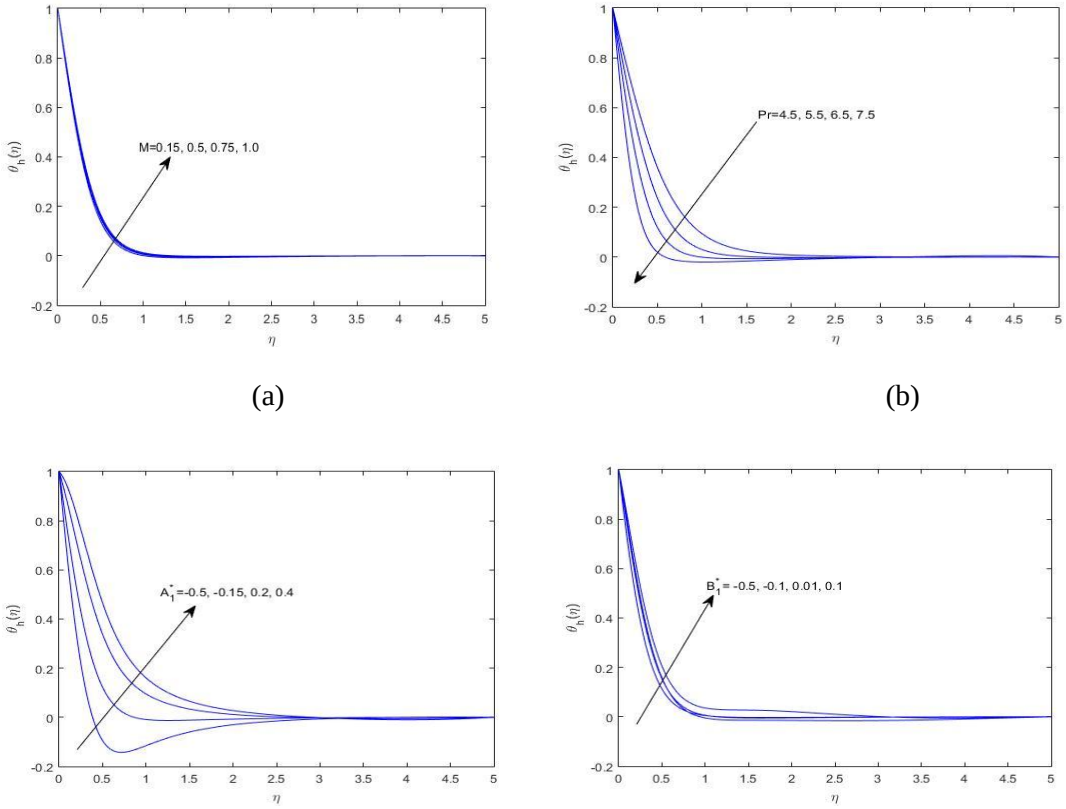

(a) (b)

(c) (d)

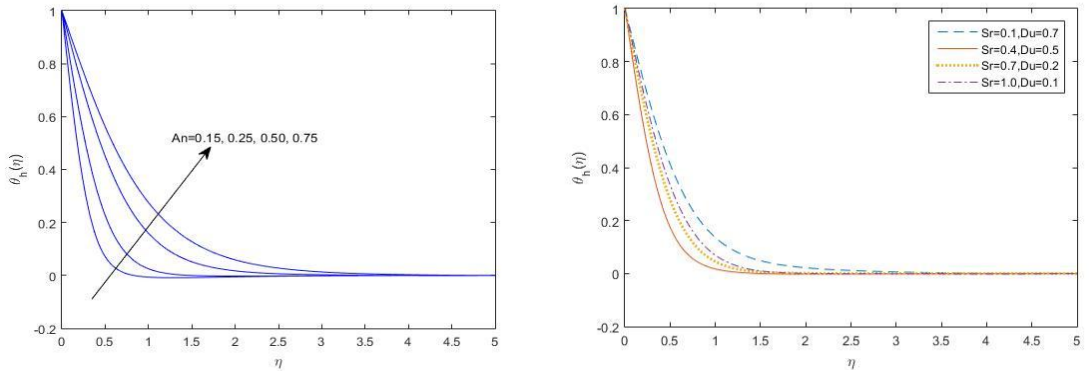

(e) (f)

Figure 3. Effects of (a) magnetic parameter, (b) Prandtl number , (c) heat source/sink (space dependent), (d)heat source/sink (temperature dependent), (e)radiation parameter, (f)soret and dufour number on the temperature profiles.

The influence of various parameters on the temperature distribution are shown in the figure 3. It can be observed from figure 3 that from all the figures the temperature is rapidly decreased and after a certain position it tends to zero. Also it is noted that there is no changes in the temperature profile. It is seen from the figure 3(a) that there is very small enhancement on the temperature profile with the increases of the magnetic parameter. From the figure 3(b) it is also depicted that the increasing values of Prandtl number leads a decreasing temperature profile. The temperature profile increases with the increases of the space dependent heat source/sink parameter which is delineated in figure 3(c). The temperature profile has an enhancement with the increment of the temperature dependent heat source/sink parameter which is displayed in figure 3(d). As depicted in figure 3(e) that the temperature profile is enhanced with the increment of the radiation parameter. The combined influence of the Soret and Dufour effect on the temperature profile is shown in the figure 3(f). From the figure it can be observe that the Soret parameter is decreased and Dufour parameter is increased. The temperature profile is decelerated with such parameter values of Sr and Du.

The impacts of various pertinent parameters on the concentration profile are represented in the figure 4. The concentration profile is increasing when $\eta \to 0$, after that it has a rapid reduction and when $\eta \to \infty$ it tends to zero. There is very small increment on the concentration profile with the enhancement of the magnetic parameter which is displayed in the figure 4(a). From figure 4(b) it can be observed that the concentration profiles decreases with the increases of the Prandtl

number. Figure 4(c) and 4(d) delineated the concentration profile with the space dependent heat source/sink parameters and temperature dependent heat source/sink parameters respectively. From both figures the concentration profiles are reduced with the increment of the heat source/sink parameters. It also be noted that there is an intersecting point which is seen in the figure 4(c), the concentration profile is proportional to the space dependent heat source/sink parameter. Figure 4(e) delineates the effects of chemical reaction parameter on the concentration profiles. From this figure, the enhancement chemical reaction parameter retards the concentration profile. The combined impact of the Soret and Dufour effect on the concentration profile is represented in the figure 4(f). From the figure it can be observe that the Soret parameter is decreased and Dufour parameter is increased. The concentration profile is enhanced for large soret paramer and small Dufour parameter value. The increment of radiation parameter improves the concentration profile which is delineated in figure 5(a).

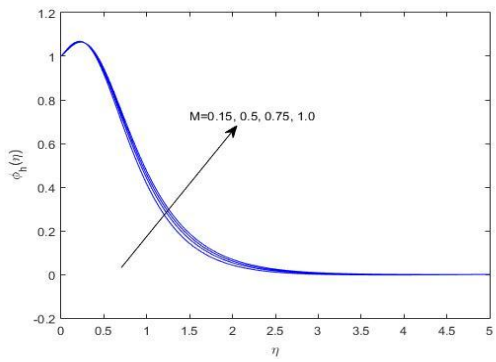

(a)

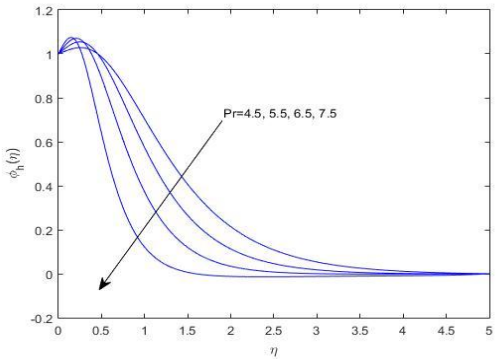

(b)

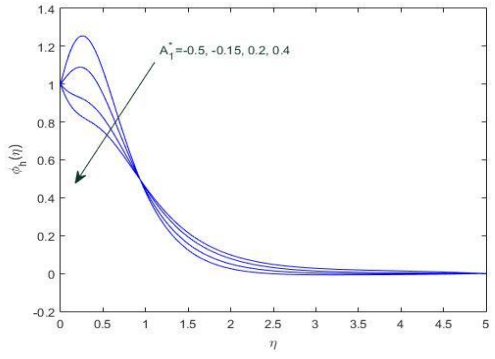

(c)

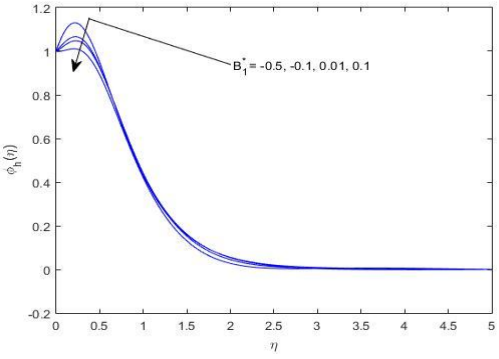

(d)

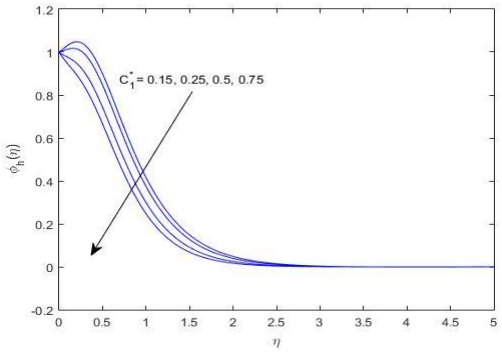

(e)

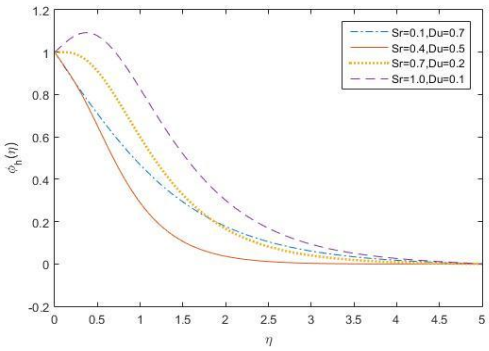

(f)

Figure 4. Effects of (a) magnetic parameter, (b) Prandtl number , (c) heat source/sink (space dependent), (d)heat source/sink (temperature dependent), (e)chemical reaction parameter, (f) soret and dufour number on the temperature profiles.

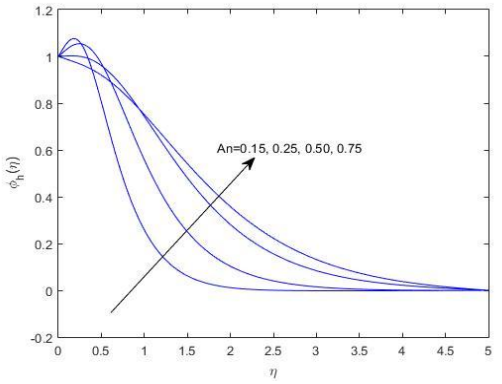

(a)

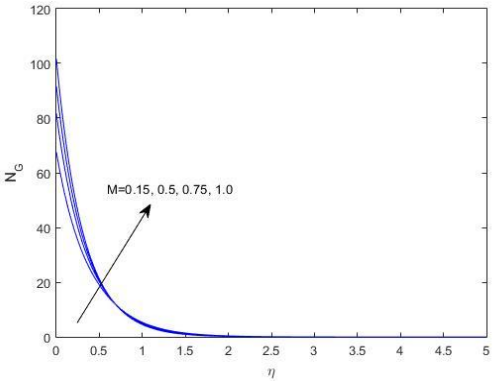

(b)

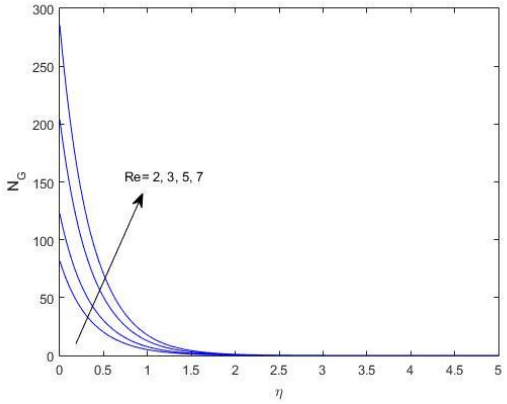

(c)

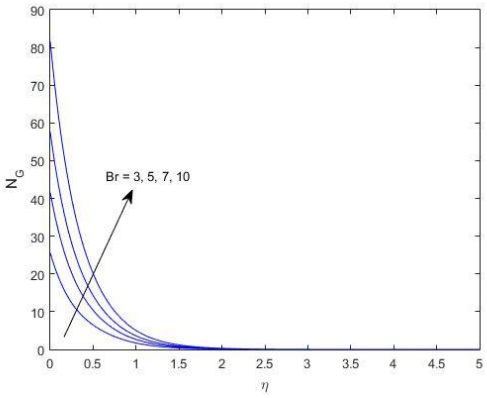

(d)

Figure 5. (a) Effects of radiation parameter on the temperature profiles. Effects of (b) magnetic parameter, (c) Reynolds number, (d) Brinkman number on the entropy generation

The Entropy generation analysis is demonstrated with the magnatic parameter, Renolds number, and Brinkman number in the figure 5(b), 5(c) and 5(d) respectively. For all cases it can be remarked that the entropy generation is decreased rapidly with respect to the position and finally it tends to zero. The entropy generation is enhanced with the increment of the magnetic parameter which is shown in figure 5(b). Figure 5(c) displays the increasing entropy generation profile with the enhancement of the Renolds number. It is also observed from figure 5(d) that the improvement of the Brinkman number enhance the entropy generation which is depicted in figure 5(d).

4. CONCLUTIONS

From this investigation , it is examined the effect of soret and duffer on the entropy generation for hybrid nanofluid for mixture of Aluminum Nitride (AIN) and Alumina nanoparticles(Al_2O_3) nanoparticles with base fluid water . The main observations of the present investigation are listed as follows:

- The temperature at fixed point decreased with increasing magnitude of soret effect but reverse results are observed when magnitude of Duffer effect is increasing.
- The concentration are different nature at near of wall and far from wall by changing the value of the magnitude of Soret and Duffer.
- The entropy generation is always increased with the other parameters.

REFERENCES

1. Tanzila Hayat, S. Nadeem, Heat transfer enhancement with Ag–CuO/water hybrid nanofluid, Results in Physics 7 (2017) 2317–2324
2. P.S. Reddy, A.J. Chamkha, Soret and Dufour effects on MHD convective flow of Al2O3–water and TiO2–water nanofluidspast a stretching sheet in porous media with heat generation/absorption, Advanced Powder Technology (2016), http://dx.doi.org/10.1016/j.apt.2016.04.005
3. M.H. Abolbashari et al., Analytical modeling of entropy generation for Cassonnano-fluid flow induced by a stretchingsurface, Advanced Powder Technology (2015), http://dx.doi.org/10.1016/j.apt.2015.01.003

4. A. Bejan, Entropy Generation Minimization: The Method of ThermodynamicOptimization of Finite-size Systems and Finite-time Processes, CRC Press,1996.
5. J.Y. San, W.M. Worek, Z. Lavan, Entropy generation in combined heat and masstransfer, Int. J. Heat Mass Transf. 30 (1987) 1359–1369.
6. K.V. Sharma, P.K. Sarma, W.H. Azmi, R. Mamat, K. Kadirgama, Correlations to predict friction and forced convection heat transfer coefficients of water based nanofluids for turbulent flow in a tube, IJMNTFTP 3 (2012) 1–25.
7. S. Cho, Effect of nitrogen flow ratio on the structural and optical properties of aluminum nitride thin films, J. Cryst. Growth 326 (2011) 179–182.